Carbohydrate Research 344 (2009) 1792–1797

Contents lists available at ScienceDirect

Carbohydrate Research

journal homepage: www.elsevier.com/locate/carres

Review

The structure of high-methoxyl sugar acid gels of citrus pectin as determined by AFM ☆

Marshall L. Fishman *, Peter H. Cooke

Eastern Regional Research Center, Agricultural Research Service, U.S. Department of Agriculture, 600 East Mermaid Lane, Wyndmoor, PA 19038, USA

ARTICLE INFO

Article history:
Received 31 July 2008
Received in revised form 17 September 2008
Accepted 18 September 2008
Available online 19 November 2008

Keywords:
Pectin
Networks
Sugar acid gels
AFM, structure
Gel strength

ABSTRACT

Images of native high-methoxyl sugar acid gels (HMSAGs) were obtained by atomic force microscopy (AFM) in the Tapping Mode™. Electronic thinning of the pectin strands to one-pixel wide allowed the pectin network to be viewed in the absence of variable strand widths related to preferentially solvated sugar. Thinned images revealed that HMSAGs of pectin comprise a partially cross-linked network, in that many of the cross-linking moieties are attached at only one end. Based on their structural similarities, aggregated pectin in water appears to be a fluid precursor of a HMSAG of pectin. Furthermore, examination of AFM images revealed that gels with 'uniform' distribution of strands and pores between strands had higher gel strengths than gels in which strands were non-uniformly distributed and were separated by large and small spaces.

Published by Elsevier Ltd.

Contents

1. Introduction

Pectin is a heterogeneous and complex polysaccharide found in the cell walls of most higher plants.[1] It is mainly a copolymer of (1–4) α-D linked galacturonic acid and its methyl ester, which is often referred to as the homogalacturonan (HG) or the smooth region of pectin. It is this region which is most abundant in pectin, particularly in citrus fruits. In the case of flash-extracted pectins from the albedo of oranges[2] and limes,[3] about 80–90% of the pectins comprised anhydrogalacturonate. Some HGs contain pendant xylose units. The second most abundant constituent in pectin is rhamnogalacturonan which contains arabinan, galactan, and arabinogalactan side chains. This region is often referred to as the hairy region of pectin. Most of the monosaccharides in pectin are found collectively in these two regions.

The most important function of pectin commercially is that it acts as a gelling or thickening agent in processed foods.[1] Thus, there has been great interest in the structure and function of high-methoxyl sugar acid gels (HMSAGs) of pectin. Current thoughts on the structure of pectin gels can be found in work reported elsewhere.[4–9] In short, it is believed that pectin gel networks form due to polymer–polymer interactions stabilized by a

☆ Mention of trade names or commercial products in this article is solely for the purpose of providing specific information and does not imply recommendation or endorsement by the U.S. Department of Agriculture.

* Corresponding author. Tel.: +1 215 233 6450; fax: +1 215 233 6406.
E-mail address: marshall.fishman@ars.usda.gov (M. L. Fishman).

0008-6215/$ - see front matter Published by Elsevier Ltd.
doi:10.1016/j.carres.2008.09.031

combination of hydrophobic interactions and hydrogen bonds and enabled by the formation of junction zones. Low-acid pH promotes hydrogen bonding between non-esterified carboxyl groups on the polysaccharide, high degrees of methylesterification of the polysaccharide promote intermolecular hydrophobic interactions, and high sugar content desiccates the polysaccharide of water enabling closer inter-polymeric contacts. The evidence to support these concepts comes from a wide variety of physical measurements.[9] Nonetheless, the development of atomic force microscope (AFM) techniques has allowed, for the first time, the visualization of HMSAG at the nanoscale level in their native state with minimal sample preparation. A detailed description of the theory of AFM and its application in biological systems is given in work reported elsewhere.[10]

2. Experimental

2.1. Material

Fresh albedo was obtained from Florida, early Valencia oranges, and Florida tropical seedless limes. Immediately upon arrival in the laboratory, the flavedo was stripped manually from the skin with a fruit and vegetable peeler, followed by removal of the albedo with a paring knife. After cutting the albedo into small pieces (ca. 1 mm^2), it was stored at −20 °C in sealed polyethylene bags until extraction. Commercial citrus pectin (MexPec 1400, degree of methylesterification, 71%) was supplied by the Grinsted Division of Danisco-Cultor (Kansas City, KS) in dry powder form and used as received.

2.2. Extraction

Two methods of extracting pectin rapidly (i.e., Flash extraction) from albedo had been described in detail previously: one method uses microwaves,[2] the other steam injection.[11] Briefly, microwave heating was performed in a model MDS-2000 microwave sample preparation system (CEM Corp., Mathews, NC). Time of irradiation was 3 min followed by rapid cooling in a cold water bath to room temperature. Extractions were in closed microwave transparent cells. After 3 min, the pressure in the cell was 30 psi and the temperature was 120 °C. Cells were loaded with 1 g of albedo dispersed in 25 mL of HCl, pH 2. Solubilized pectin was precipitated with 70% isopropyl alcohol (IPA), washed once with 70% IPA and once with 100% IPA. The sample was dried by vacuum at room temperature and stored in screw-capped vials until further use.

Flash extraction of orange albedo pectin by steam injection heating had been described previously.[11,12] The closed extraction vessel was a modified bacteria fermenter capable of producing 30 g batches of pectin. Five gallons of pH 2.0 nitric acid (HNO_3) were preheated to 95–100 °C, followed by the addition of 774 g of wet albedo. Then, the temperature was raised to 110 °C and held there for 3 min. Next, the sample was rapidly cooled using an in line cold water heat exchanger and filtered through miracloth. The pectin was precipitated by adding 11.4 L of 70% IPA to supernatant. The supernatant was stirred and allowed to stand at room temperature for 1/2 h, followed by filtering. The recovered pectin was washed with 4 L of 100% IPA and placed in freezer overnight before being vacuum dried the next day.

2.3. Preparation of gels and determination of gel strength

Preparation of gels and measurement of gel strength had been described previously.[12,13] Final composition (w/w) of the gels was 0.25% pectin, 65% sucrose, and 35% buffer. The pH of the buffer was controlled by the molar ratio of citric acid and sodium citrate. Gel strength (force which ruptured the gel) was determined with a Stable Microsystems TA-XT2 Texture Analyzer.

2.4. Atomic force microscopy

For solution studies, samples were dissolved in HPLC grade water and were serially diluted to the desired concentration. Two microliters of the solution were pipetted onto a freshly cleaved 10 mm diameter disk of mica and were air dried. The mica was mounted in a Multimode Scanning Probe microscope with a Nanoscope IIIa controller, operated as an atomic force microscope in the Tapping Mode (Veeco Instruments, Santa Barbara, CA). A concentration-dependent dispersion of pectin adhering to the mica surface was scanned with the AFM operating in the intermittent contact mode using tapping mode etched silicon probes (TESPs). Additional information concerning the AFM and its operation can be found in work reported elsewhere.[12,13]

In the case of sugar acid gels, a thin (1 mm) slice of transparent gel was cut manually from the gel with a stainless steel razor blade. A freshly cleaved 10 mm diameter disk of mica was applied to the cut surface of the gel. After 5–10 min, the disk was peeled off the gel surface (peel-transfer) and mounted in the AFM.

Selected images were analyzed by software version 5.12 rev. B which is described in the Command Reference Manual supplied by the manufacturer. Length, widths, and areas were determined by particle analysis. For individual molecules in dilute solution, this process is straightforward. In the case of gels objects of interest (OOI), that is, strands and pores, the OOI must be separated from other objects by a process called threshold segmentation. To accomplish this, we chose a threshold value for pixel intensity which removed or masked the intensity of background pixels and allowed the pixel brightness of OOIs to remain undiminished. Prior to particle analysis, lowpass filtering was applied to reduce background noise; in some cases, high pass filtering was applied to highlight the OOIs which are delineated from the background as areas of rapidly changing height or phase.

Repeatedly during the course of AFM experiments, the cantilever was tuned to resonance by a feature of the manufacture-supplied software called autotune. This feature automatically centers the phase so that the phase-shift will always be positive (brighter).

3. Results and discussion

Several years ago, we demonstrated by electron microscopy that peach pectin when imaged from dilute aqueous solution formed network structures,[14,15] and the networks could be dissociated into their component parts by the addition to the solution of 50% glycerol or 5–50 mM NaCl. This provided direct evidence for the role of hydrogen bonds in network formation. These studies have led us to suggest that possibly, the networks in the solution were precursors to the networks formed in HMSAG of pectin. More recently (see Fig. 1), we were able to show by AFM that orange pectin when imaged from dilute aqueous solution formed network structures similar to those formed by peach pectin.[13] Although, the AFM images required far less sample preparation than those from electron microscopy, both samples were dehydrated when imaged.

In the case of HMSAG of pectin, we were able to obtain their AFM images in the hydrated state simply by scanning over the hydrated gel which was thinly layered on freshly cleaved mica. Figure 2A and B are images of commercial citrus pectin obtained from such an experiment. In TappingMode AFM, the cantilever is excited into resonance oscillation with a piezoelectric driver. Figure 2A is a height image generated by the rise and fall of the AFM cantilever as the probe tip scans over the surface of the gel in soft tapping mode.

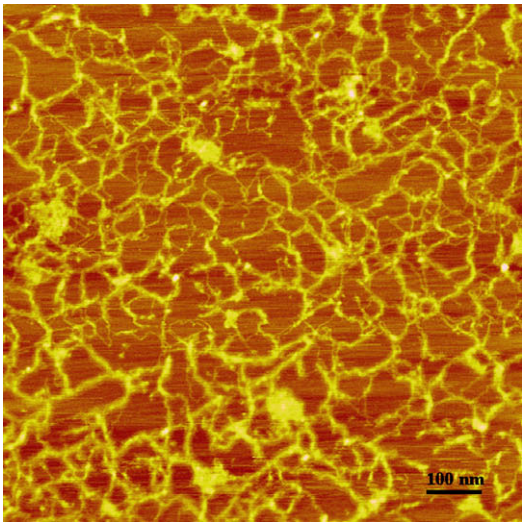

Figure 1. Height image of pectin dissolved in water, concentration 13.1 μg/mL deposited on mica, air dried. Reprinted from Ref. 12.

Figure 2B, the phase-shift image, is generated simultaneously due to phase lag between the wave form of the vibrating AFM cantilever as the probe tip scans over the sample and the wave form of the drive. Comparison of Figure 2A and B reveals that the two images are related to one another in the same way as a positive and a negative of a photograph taken with film are related to each other. Furthermore, Figure 2A reveals that the strands of the gel (indicated by the brown color) are clefts in the interstitial fluid. If the strands were above the interstitial fluid, they would be of the same color as those in 2B. Immediately after peel transfer of the gel on mica, the contrast between strands and the interstitial fluid gradually fades until the strands are barely visible. This phenomenon is due to the height of the interstitial fluid decreasing which results in a flattening of the sample. Because the strands are in a cleft, it is not possible to measure their height. Nonetheless, even though the gel has flattened, there is still sufficient delineation between strand and interstitial fluid to produce phase-shift images with good contrast. The contrast is due to a difference in interactions between probe and strand as compared to probe and interstitial fluid.

We believe that 'clefts' beneath the surface of the interstitial fluid resulted from the method of sample preparation and were marked by their dark appearance in height images. Image interpretation was guided by repeatable, experimental observations as well as some theoretical considerations of the instrumental mechanism of image formation; the appearance of prominent cleft-like depressions in the height image was always a diminishing transient, lasting upwards of 30 min of continuous scanning (in contrast to the persistent phase-shift image lasting for a few hours). As described in earlier publications, a scoop of the free-standing, solid gel was cut or dissected with a stainless steel razor blade into a millimeter thin slab, then the surface of the slab was 'peeled' onto mica mounted on a metal disk. Peel transfer describes the process of gently setting the mica attached to the sample disk on the gel slab and gently lifting it off. Those preparative actions together are likely to produce a fresh thin layer of the gel on the mica which was immediately scanned under ambient conditions in air. We reasoned that the viscous interstitial phase of the gel might be lifted by the mechanics of the preparative steps into slightly elevated levels above the more dense strands of pectin, and was then slowly relaxed to a position that was in level with the network of strands.

An alternate interpretation of the dark strands in the height image is based on the assumption that there is larger damping of the cantilever amplitude in the porous interstitial phase of the gel over damping of the cantilever amplitude in the pectin strand phase. This phenomenon might occur if there is capillary adhesion of the probe tip in the fluid phase but little or no adhesion of the tip in the phase containing pectin strands if the strands were fibrous and dry. It has been found elsewhere that at the high set-point ratio (0.95) used in this study, the phase image obtained is dominated by adhesion forces between the surface and the probe tip rather than repulsive forces as would be true if the strands were hard and dry and the set-point ratio was less than 0.6.[16,17] In view of the high concentration of sucrose present, the vapor pressure of the buffer solution is expected to be low and consequently, evaporation of solvent is expected to be low which accounts for the minimal evaporation of solvent which we observed during the time frame of AFM imaging. Because sucrose is dissolved, we hypothesize that the fluid behaves like a binary solvent of two hydrogen bonding components in the presence of a glucan, namely water and sucrose in the presence of pectin. It has been shown elsewhere that in such systems, if one of the solvating agents is greatly in excess of the other, then the excess agent will preferentially solvate the glucan.[18] Thus, in the case of HMSAG, pectin will be coated with a 'sticky' layer of buffer and sucrose in which the concentra-

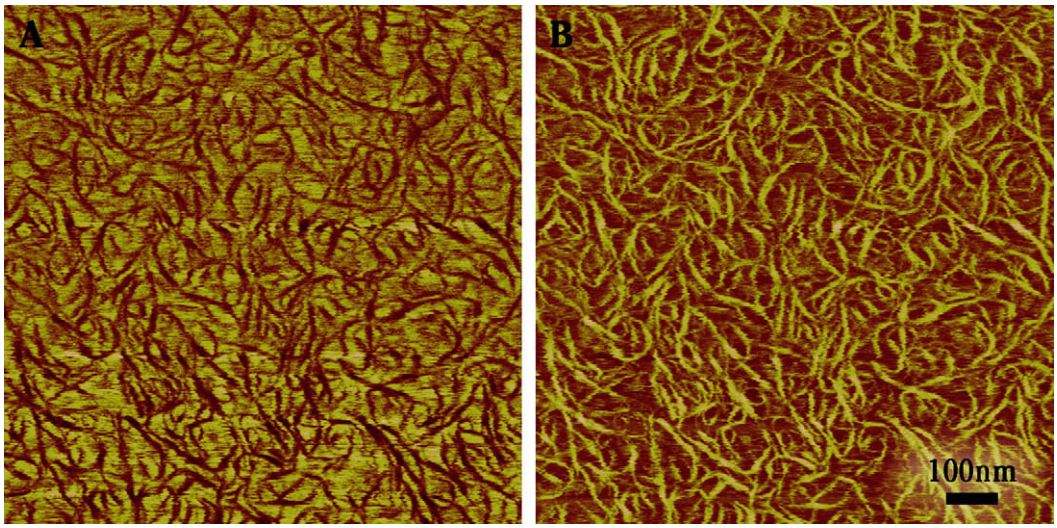

Figure 2. Matching images of (A) height and (B) phase-shift of an acid gel made from commercial citrus pectin (CCP). The organization of thin clefts or depressions in the surface of the gel in (A) corresponds to the arrangement of phase-shifted areas in (B). Reprinted from Ref. 13.

tion of sucrose in that sticky layer will be higher than in the overall solution and more importantly in the interstitial phase. Hence, the phase-shift of the oscillating cantilever will be greater when scanning over the pectin strands than when scanning over the interstitial space due to greater adhesion between pectin phase and tip than between interstitial phase and tip. Since the phase angle was found to be constant while scanning the sample, it is reasonable to assume that evaporation of water in the sample is not significant.

Figure 3 contains phase-shift images of commercial citrus pectin (CCP), orange albedo pectin (OAP), and lime albedo pectin (LAP). For purposes of comparison, gels were made at the pH value which gave optimum gel strengths at break. LAP gave a value of 9.1 KPa (117 g) at pH 3.53; OAP gave a value of 8.3 KPa (107 g) at pH 3.23, and CCP gave a value of 6.7 KPa (87 g) at pH 3.00. Tables 1 and 2 contain molecular dimensions of gel segments obtained by threshold segmentation for the gels in Figure 3. Dimensions of 100 of the largest gel segments and 100 of the largest pores obtained from phase images are given in Table 1. Area, length, and width dimensions are smaller for LAP than for either OAP or CCP. All three pectin sources gave about the same dimensions for pores. Comparable dimensions of strands are larger than those of pores. Height measurements on individual OAP molecules by AFM gave a value of about 4.3 ± 0.03 nm.[12] In this study, width measurements on large strands gave average values of about 28 nm for CCP and OAP gels, and about 20 nm for LAP gels. If we assume that the width of a sugar molecule is about 0.5 nm, as many as 47 sugar molecules could be immobilized laterally to a single large pectin molecule. Even if as indicated by studies in dilute solution[14,19] that as many as four pectin molecules are aggregated in a strand, the total number of laterally immobilized sugars would change only slightly.

Dimensions of the strands and pores for the entire field are given in Table 2. These numbers were obtained from 3 phase images for each kind of gel. In the case of strands, fields were averaged from 3004, 2848, and 4222 objects for CCP, OAP, and LAP, respectively. For pores, fields were averaged from 4551, 4947, and 5852 objects for CCP, OAP, and LAP, respectively. Comparison of the data in Tables 1 and 2 reveals that there are many more barely visible small segments in the sample than there are large segments. The ratio of strand to interstitial area for CCP, OAP, and LAP is 0.83, 0.77, and 0.87, respectively, for the entire field. The percentage of the whole field area which is polymer is 45%, 43%, and 46% for CCP, OAP, and LAP, respectively. The last finding is rather remarkable if one considers that the ratio of sucrose to pectin (w/w) is 260:1. If one assumes that the strands comprise a pectin framework holding bound or immobilized sucrose and that the bound sucrose is proportional to the strand area, then the ratio of bound sucrose to pectin will be in the range of 112:1–120:1.

In any study involving imaging by AFM, one must consider the effect of probe sample interactions on the molecular dimensions that are obtained. An important artifact which requires consideration is over- or underestimating molecular dimensions of the molecules under examination. The tapping mode probes used in this study are pyramidal in shape. If the molecule which is being measured sits on a surface, the side of the probe will cause the tip to rise before it reaches the leading edge of the molecule and to fall after it passes over the trailing edge of the molecule. In that case, the measured dimension will be larger than the actual dimension. This effect has been termed 'probe broadening'.[10] If the molecule sits in a cleft or a well below the surface, the tip will not reach the bottom of the cleft until it has passed the leading edge of the molecule. Furthermore, the tip will rise prior to reaching the trailing edge of the molecule. In that case, the measured dimension will be smaller than the actual dimension. This effect could be termed 'probe narrowing'. In Figure 2, we clearly demonstrate that the strands are in a cleft below the surface of the interstitial fluid (pores). Thus, it is possible that we underestimated the area and width of the strands and overestimated the area and width of the pores. The flatness of the sample and the high setpoint ratio (about 0.95) employed in this study should work to mitigate the effects of these artifacts.

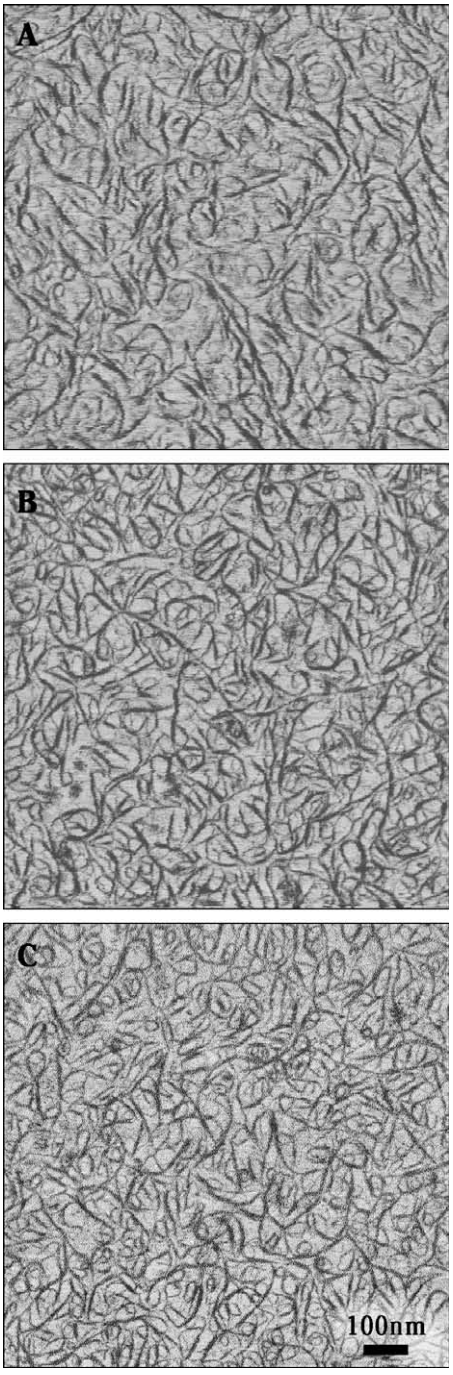

Figure 3. Comparison of phase-shift images of acid gels from three sources. (A) commercial citrus pectin, (B) orange albedo pectin, (C) lime albedo pectin. Reprinted from Ref. 13.

Figure 4A–C, images of CCP, OAP, and LAP, respectively, were obtained by electronically thinning strands of phase images such as those shown in Figures 2B and 3. The strands in these images were thinned to a width of 1 pixel. These images reveal that the presumed pectin framework in the absence of sucrose is a partially cross-linked network (PCN) in that many of the potential cross-

Table 1
Dimension of 100 largest gel segments[a]

Sample	Strands			Pores		
	Area (nm^2)	Length (nm)	Width (nm)	Area (nm^2)	Length (nm)	Width (nm)
CCP	1598 (126)	118 (3)	27.6 (2.5)	703 (98)	70.1 (4.9)	14.2 (2.8)
OAP	1734 (84)	119 (4)	28.6 (2.7)	629 (37)	64.7 (3.8)	12.8 (0.6)
LAP	1107 (208)	100 (6)	19.8 (1.2)	514 (127)	56.8 (6.0)	11.6 (2.5)

Reprinted from Ref. 13.
[a] Numbers in parentheses are standard deviations of triplicate analysis.

Table 2
Dimension of entire field of gel segments[a]

Sample	Strands			Pores		
	Area (nm^2)	Length (nm)	Width (nm)	Area (nm^2)	Length (nm)	Width (nm)
CCP	260 (9)	28.0 (0.7)	7.88 (0.22)	207 (29)	22.0 (6.0)	7.80 (0.76)
OAP	254 (40)	27.8 (1.7)	7.76 (0.61)	190 (20)	25.1 (1.4)	7.49 (0.45)
LAP	183 (32)	25.1 (0.8)	6.57 (0.44)	152 (33)	21.7 (2.5)	6.91 (0.73)

Reprinted from Ref. 13.
[a] Numbers in parentheses are standard deviations of triplicate analysis.

linking moieties have linked only at one end. Visual examination reveals that the density of molecules in the PCN is somewhat greater for LAP gels than for OAP or CCP gels. The greater number of objects in LAP gels over CCP or OAP gels is consistent with a higher pectin density for LAP as compared with either CCP or OAP. We note that there are several similarities between the images in Figure 4 and previously rotary-shadowed images of peach pectin[14] from dilute aqueous solutions of 0.005 M NaCl. In the cases of both the peach and the citrus, the networks are a collection of mostly open branched structures. All but a few of the branches are tri-functional. Furthermore, all structures comprised rods, segmented rods, kinked rods, or combinations of these elements linked at their ends. Although some of the branched points could be construed as arising from junction zones, a significant number of branch points occur at right angles. These could arise from the joining of individual functional groups such as hydrogen bond formation between oxygen from carboxyl groups, OH groups, or glycosidic bonds and hydrogens from carboxyls and OH groups. This picture is in sharp contrast to the appearance of the gels when the adsorbed sugars are visualized, for example, Figures 2 and 3. In this case, most branched points appear to be formed from 'cooperative junctions whose stability depends on the specific energy of the linkages and the number of units cooperatively bound'.[20] One might infer from these images that the adsorbed sugar molecules function as a coating which aids in strengthening branch points, possibly through cooperative interactions.

Recently, Lögren et al.[7] imaged thin sections of HMSAG cross-linked with glutaraldehyde, stained with ruthenium red, and dehydrated for imaging by transmission electron microscopy. They imaged areas which were in the range of 0.5–4 μm^2, whereas our fields were 1–25 μm^2. They described open networks with many pores greater than 0.5 μm in diameter, and the strands were aggregated in bundles or in loose aggregates and branched in an irregular pattern. Furthermore, they suggested that there was a tendency toward parallel alignment of strands and that strands appeared stiff and straight.

Our direct images of native gels (Fig. 4A–C) revealed a uniformly distributed PCN of strands in which strands appear branched and stiff. As mentioned previously, in addition to straight rodlike strands, our images reveal curved and kinked strands (segmented rods and kinked rods). Rees and Wight[21] predicted that pectin

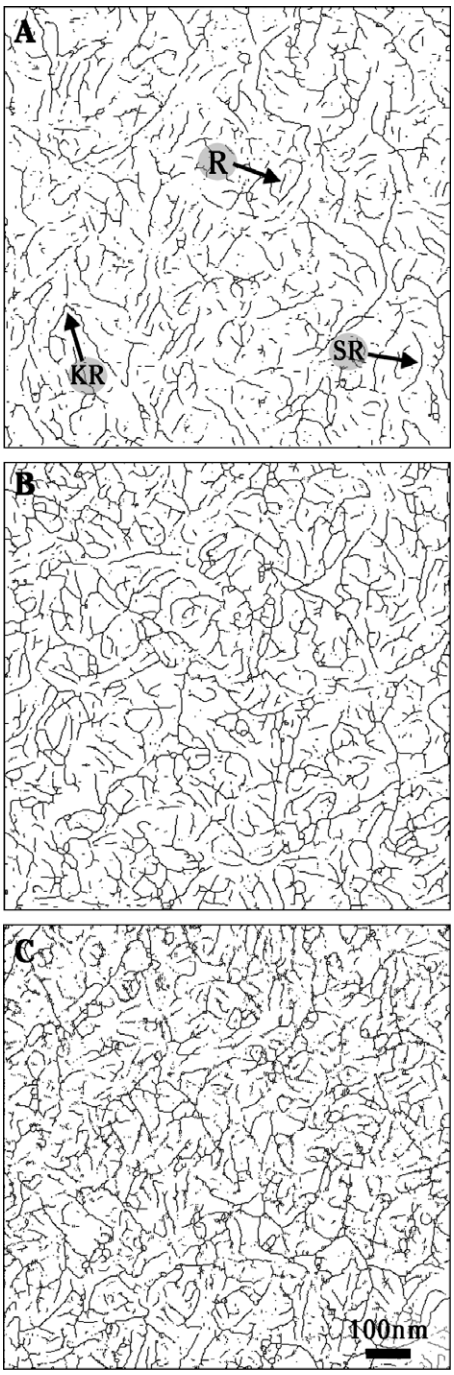

Figure 4. Electronically thinned strands from phase images of gels. (A) Commercial citrus pectin, CCP; (B) orange albedo pectin, OAP; (C) lime albedo pectin, LAP. Images appear to reveal pectin framework in the absence of sucrose. Joined structures within the frame work are combinations of rods (R), segmented rods (SR), and kinked rods (KR). Reprinted from Ref. 13.

molecules would kink at points where rhamnose was located in the pectin backbone based on NMR measurements in combination with modeling studies. As indicated by differences in height images, that is, strands that are below and flush with the surface of the interstitial fluid, the gel appears quite fluid. In contrast, the components of the PCN's appear quite stiff. In fact, the networks may be quite deformable in that they are partially cross-linked and held together by secondary forces, for example, hydrogen bonds and van der Waals forces, which may break when subjected to pressure and reform when the pressure is released.

This could be the basis of pectin's unique ability to form spreadable gels.

In Table 1, the average pore length for 100 of the largest pores from the three kinds of gels ranged from about 57–70 nm, the average pore width from about 12–14 nm and the average pore area from about 514–703 nm^2. Table 2 contains averages of all pores in a 1 μm^2 area. In this case, average lengths are about 23 nm, widths about 7.5 nm and areas about 183 nm^2. Also worthy of note is that comparison of images of structures in a 1 μm^2 area with those in a 25 μm^2 area (image not shown) revealed that in both cases structures are uniformly distributed.

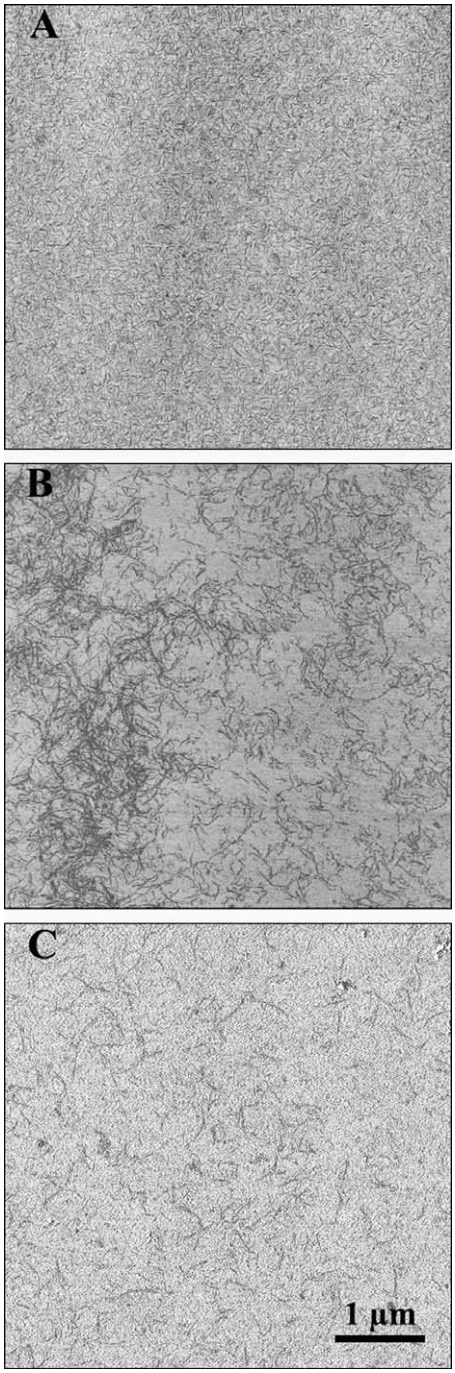

Figure 5. Phase images of pectin high-methoxyl sugar acid gels. Pectin prepared by steam injection. Thin layer of gel smeared on mica. (A) pH 3.41, gel strength (g) 96; (B) pH 3.03, gel strength (g) 29; (C) pH 2.86, gel strength (g) 11. Reprinted from Ref. 12.

A plot of the force at which the gel ruptured (sometimes referred to as gel strength at break in the literature) against pH of the buffer strength used in making a HMSAG of pectin can be fitted to a Gaussian curve.[12] With the intention of correlating gel structure with gel strength at break, we investigated by AFM of the structure of three gels in which gel strength was varied by changing the pH of the buffer in which the pectin and sugar were dissolved. Images generated in that study are shown in Figure 5A–C. The three gels shown in Figure 5 were made with buffer pHs of 3.41(A), 3.03(B), and 2.86(C) and had gel strengths of 96 ± 8 g, 29 ± 1 g, and 11 ± 1 g, respectively. It appears from visual examination of the gels images that uniform distribution of strands and minimal space between strands may be important factors in determining gel strength. The strands in the gel which is imaged in Figure 5A are distributed uniformly, and there is minimal space between strands whereas the strands in Figure 5B are non-uniformly distributed and appear to be tangled rather than in a network structure. In Figure 5C, large strands appear to be separated by large spaces.

4. Conclusions

Based on structural similarities, aggregated pectin in water appears to be a fluid precursor of a HMSAG of pectin. The role of sugar in HMSAG of pectin may be to fix pectin strands in a metastable state by preferential solvation of the pectin network arising from the high concentration of sugar present. Electronically thinning of pectin strands to one-pixel width produced a view of the pectin framework stripped of sucrose. Based on these images, it appears that pectin in HMSAG is a partially cross-linked network in that many of the cross-linking moieties are attached at only one end. This partial cross-linking of the pectin strands may be related to the relative fluidity of HMSAG of pectin as compared to other gels. Gel strength appears to be correlated to the density of pectin strands and to the uniformity of pectin distribution within the gels.

References

1. Schols, H. A.; Voragen, A. G. J. In *Pectins and their Manipulation*; Seymour, G. B., Knox, J. P., Eds.; Blackwell Publ. Ltd: Oxford, UK, 2002; pp 1–29.
2. Fishman, M. L.; Chau, H. K.; Hoagland, P.; Ayyad, K. *Carbohydr. Res.* **2000**, *323*, 126–138.
3. Fishman, M. L.; Chau, H. K.; Hoagland, P. D.; Hotchkiss, A. T. *Food Hydrol.* **2006**, *20*, 1170–1177.
4. Jarvis, M. In *Pectins and Their Manipulation*; Seymour, G. B., Knox, J. P., Eds.; Blackwell Publ. Ltd: Oxford, UK, 2002; p 130.
5. Tsoga, A.; Richardson, R. K.; Morris, E. R. *Food Hydrol.* **2004**, *18*, 907–919.
6. Tsoga, A.; Richardson, R. K.; Morris, E. R. *Food Hydrol.* **2004**, *18*, 921–932.
7. Lögren, C.; Walkenström, P.; Hermansson, A. *Biomacromolecules* **2002**, *3*, 1144–1153.
8. Löfgren, C.; Guillotin, S.; Evenbratt, H.; Schols, H.; Hermansson, A. *Biomacromolecules* **2005**, *3*, 1144–1153.
9. Oakenfull, D. G. In *The Chemistry and Technology of Pectins*; Walter, R. H., Ed.; Academic Press Inc.: San Diego, CA, 1991; pp 87–118.
10. Morris, V. J.; Kirby, A. R.; Gunning, A. P. *Atomic Force Microscopy for Biologists*; Imperial College Press: London, 1999.
11. Fishman, M. L.; Walker, P. N.; Chau, H. K.; Hotchkiss, A. T. *Biomacromolecules* **2003**, *4*, 880–889.
12. Fishman, M. L.; Cooke, P. H.; Chau, H. K.; Coffin, D. R.; Hotchkiss, A. T., Jr. *Biomacromolecules* **2007**, *8*, 573–578.
13. Fishman, M. L.; Cooke, P. H.; Coffin, D. R. *Biomacromolecules* **2004**, *4*, 334–341.
14. Fishman, M. L.; Cooke, P.; Levaj, B.; Gillespie, D. T. *Arch. Biochem. Biophys.* **1992**, *294*, 253–260.
15. Fishman, M. L.; Cooke, P.; Hotchkiss, A.; Damert, W. *Carbohydr. Res.* **1993**, *248*, 303–316.
16. Maganov, S. N.; Elings, V.; Whangbo, M.-H. *Surf. Sci.* **1997**, *375*, L385–L391.
17. Kioussis, D. R.; Kofinis, P. *Polymer* **2005**, *46*, 10167–10172.
18. Brant, D. A.; Straub, P. R. *Biopolymers* **1980**, *19*, 639–653.
19. Fishman, M. L.; Pepper, L.; Pfeffer, P. E. In *Water Soluble Polymers: Beauty with Performance*; Glass, J. E., Ed.; American Chemical Society: Washington, 1986; Vol. 213, pp 57–70.
20. Rinaudo, M. In *Pectin and Pectinases*; Voragen, A. G. J., Visser, J., Eds.; Elsevier: Amsterdam, Netherlands, 1996; pp 21–33.
21. Rees, D. A.; Wight, A. W. *J. Chem. Soc. (B)* **1971**, 1366–1372.